NASA-TM-112323

Reprinted From
NDE — Vol. 5, Nondestructive Evaluation:
NDE Planning and Application
Editors: R. D. Streit, H. Takahashi, F. B. Stulen
T. Seiwert, D. Cowfer, J. Cook, and A. Green
Book No. H00468 — 1989

The American Society of Mechanical Engineers

COMPARISON OF RESIDUAL STRESS MEASUREMENTS IN WELDED THIN PLATES BY X-RAY AND HOLE DRILLING METHODS

R. W. Hampton, Research Engineer
Test Engineering and Analysis Branch
NASA Ames Research Center
Moffett Field, California

D. V. Nelson, Associate Professor
Mechanical Engineering Department
Stanford University
Stanford, California

ABSTRACT

Welding induced residual stresses are frequently of interest in fracture evaluations of critical components. Although some data are available on surface and interior stresses of welded plates, data for commonly used materials with a comparison of different measurement techniques, and in particular for thin plate applications, are sparce. This paper provides the results of an investigation of residual stresses in thin butt-welded steel plate specimens. Longitudinal stress profiles are reported across the 102 mm width of longitudinal and transverse welded test specimens using both the x-ray diffraction and strain gage hole drilling methods, which are compared. Data are given on the variation of stresses with depth in the specimen.

NOMENCLATURE

D = Gage pattern mean diameter = 2*rm
D0 = Hole diameter
E = Young's Modulus
rm = Gage pattern mean radius
T = Thickness of plate
W = Width of plate
X = Transverse direction as shown in Fig. 1
Y = Longitudinal direction as shown in Fig. 1
Z = Depth of hole
σ_i = Stress in direction i
υ = Poisson's Ratio
ζ = Distance from neutral axis of reduced thickness section
Ψ = Angle between surface normal and x-ray beam bisector

INTRODUCTION

Welding induced residual stresses are frequently of interest in fracture evaluations of critical components (e.g., see Kula and Weiss, 1982, ASTM STP 776, and Dittman et al., 1987). Both surface and interior stresses are needed, and have been measured by several methods including the x-ray diffraction technique (Rudd et al., 1985) and the strain gage hole-drilling method using incremental drilling (Nickola, 1986, 1984). (An evaluation and development of the hole drilling methodology for applications with thin plate weldments such as those described here is given in a companion paper by Hampton and Nelson, 1989). The purpose of this paper is both to provide data on surface and interior residual stresses in thin welded plates, and to compare the results obtained by the x-ray and hole drilling methods for the same plates.

EXPERIMENTAL APPROACH

Specimen geometry used in the experimental investigation is shown in Fig. 1. Three types of specimens were used: plain (no welds, P), longitudinal (L) welded specimens, and transverse (T) welded specimens. The material used was ASTM A 516-70, 6.35 mm thick steel plate. To minimize previous fabrication stresses, the plate was stress relieved at 1150 F, as per standard AWS D1.1 (1987), (in a reducing atmosphere to minimize material loss) before welding and machining to size. The resulting plate material was found to have an ASTM grain size of 10 (11 mm) and tensile properties from coupon tests as shown in Table 1.

Table 1. Specimen Material Data.

Young's Modulus:	2.07×10^5 MPa
Poisson's Ratio:	0.28
Upper Yield Point:	490 MPa
Lower Yield Point:	448 MPa
Ultimate Strength:	683 MPa
Elongation (5 cm):	26 %
Reduction of Area:	63 %

Specimens were machined to rough shape before welding so that subsequent machining would not significantly change their cross-sectional shape and affect the residual stress equilibrium. Welds were made by a machine gas metal arc welding process to obtain as uniform a residual stress field as possible. A straight weld preparation with a gap of 2.5 mm resulted in a weld width of 5 mm. Two welding passes were used, one from each side with back gouging before the second pass. Details of the welding parameters are given in Table 2. The hardness of the plate tensile coupons and the welded specimen plate material was 85 R_B. Hardness of the weld and the heat-affected-zone was 89 R_B.

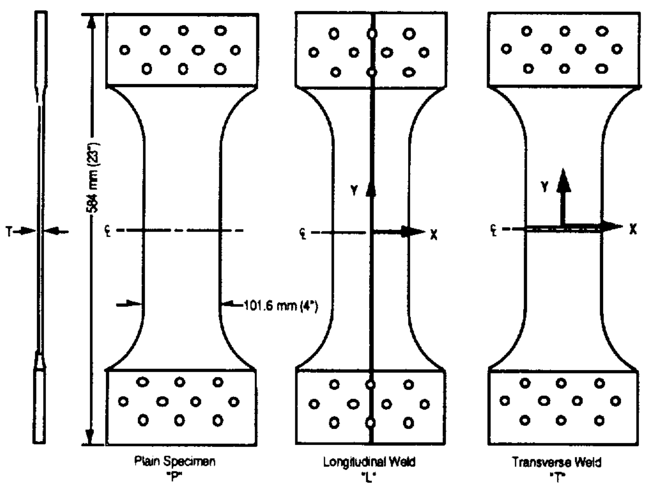

Fig. 1 Specimen Geometry

Table 2. Specimen Welding Details.

Welding Process: GMAW, 1.1 mm AWS A 5.18 (ER 70 S-3) wire.

Pass	Volts	Amps	Wire Feed	Travel Speed	Heat Input
1	20	150	650 cm/min	28 cm/min	6.5 KJ/cm
2	22	140	584 "	41 "	4.6 "

After welding, specimens were machined to their final shape. Warpage was minimized by restraint of the specimens during welding; however, the as-welded specimens were not flat. Since the specimens could not be straightened without affecting the welding residual stresses, sanding was used in conjunction with machining and grinding to obtain the thicknesses used for stress measurements shown in Table 3. As discussed in the companion paper, and by Prevey (1988), it was necessary to remove stressed surface material resulting from sanding and other final operations by chemical milling 0.13 mm from each surface before either type of stress measurements were made on specimens L1 and T1.

Table 3. Specimen Sizes and Data Listing.

Spec.	T	Specimen Data					Stress Data Fig.	
	(mm)	Gage	Z/rm	Z/D0	T/D0	T/Z	Strain Gage	X-Ray
1P	5.18	031RE	0.891	1.18	5.37	4.5		
1P	5.18	062UM	0.842	1.22	2.91	2.4		
1P	2.67	062UM,RK	0.545	0.79	1.50	1.9	2	
L1	5.84	062UM	0.545	0.79	3.29	4.2	5,6	3,5
L1	2.34							3,6
T1	5.87	062UM	0.545	0.79	3.30	4.2	7,8	
T1	2.57							4,7,8

Longitudinal (Y direction) stresses were measured across the 101.6 mm width (X direction) at the center of the specimens (Fig. 1) by both the strain gage hole-drilling method and the x-ray diffraction technique. The transverse, "T," specimen measurements were made along the weld heat-affected-zone region. The opposite sides of the plates are referred to as the "A" and "B" sides. Other details on the specimen experiments reported in this paper and the companion paper are given in Table 3.

X-RAY MEASUREMENTS

For comparison to the strain gage results presented later, x-ray diffraction residual stress measurements were made on the same specimens. The basic methodology for this technique is covered in many references (e.g., Hilley, 1972, and Kobayashi, 1987) and will not be repeated here, except to note that since the x-ray method only acquires data to a small depth (nominally 0.01 mm), it is vital to remove any extraneous material at the surface which has been mechanically deformed by machining operations. This was accomplished by the previously described chemical milling (which also provided a stress-free surface for the strain gage hole drilling measurements described later.)

The x-ray equipment used was a position-sensitive detector system which was able to acquire data from these large specimens. During preliminary setup studies, it was determined by trial and error that the setup parameters given in Table 4, with two degrees of oscillation (as discussed by James, 1987) provided data with the lowest errors.

Table 4. X-Ray Setup Parameters.

Collimator:	1.5 mm rectangular slit
X-ray target:	Chromium, l=2.29092A
Detector Bragg Angle:	156 deg.
Ψ oscillation angles:	2 deg.
Voltage, beam current:	35 KV, 1.25
Peak bounding range:	20.%
Stress spectra count time:	125 sec.
Ψ angles:	9 from -30 to 30 deg.

The x-ray technique was used to provide a fine resolution of the residual stress distribution. Data were taken for a minimum of every 5.1 mm for the center 50.8 mm on side "A," and changing to a 8.4 mm spacing for two more steps toward both edges, with a final measurement 3.2 mm from each edge. On side "B," a spacing of 10.2 mm was used to minimize the number of x-ray measurements required and to match the strain gage data locations. This resulted in a minimum of 24 measurements on each specimen at one thickness.

X-Ray Calibrations

As part of the setup, a value for the factor $(1+\upsilon)/E$ is needed, but the Poisson's ratio and Young's modulus must be evaluated for the particular x-ray diffracting crystallographic plane used. One method for measuring this parameter using a beam in 4 point bending is discussed by Prevey (1977). A slightly different procedure was used here.

Two sample A516-70 strips were made from an "L" specimen: beam "1" representing the "as is" L specimen, and beam "2" which received another stress relief treatment (to study the effect of heat treatment on the elastic constants). The beams were cut out so as to include the weld region, and so that they would fit easily into a cantilevered bending calibrator. A micrometer was used to produce differential deflections at the end of the beam, and a simple fixed-ended beam formula was used to compute the induced stress in the beam. The x-ray system was configured to acquire data using the setup for a similar iron material with a close, but not exact $(1+\upsilon)/E$ factor, which resulted in computation of "apparent" x-ray stresses from the strain data instead of actual stresses. The resulting applied stresses versus the apparent stresses were plotted as shown in Fig. 2 to obtain a correction factor from the slope of the data, ignoring the upper end points where yielding has changed the linearity.

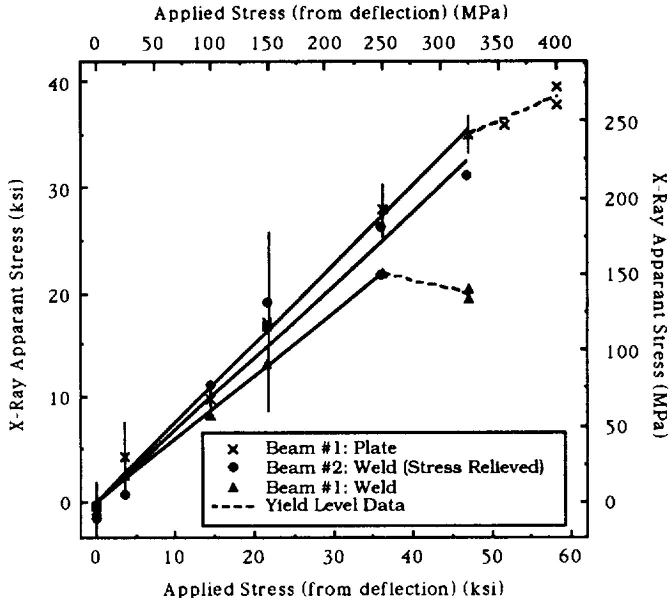

Fig. 2 X-ray calibration data.

The vertical lines in Fig. 2 are the error bands for beam #1, plate data, as determined by the x-ray equipment computer software that evaluates the "Goodness of Fit" of a linear equation to the x-ray diffraction data for the various Ψ angles used, as well as statistical counting errors. It is clear from the agreement of the data points that the stresses computed from the linear equation fit are much better than indicated by the error bands. The elastic constant factors for stresses below yield level were computed using the slope corrections as:

Material:	plate	weld	stress-relieved weld
$(1+\upsilon)/E$: $(MPa)^{-1}$	$4.80 * 10^{-6}$	$3.83 * 10^{-6}$	$4.39 * 10^{-6}$

The difference between these experimental values for $(1+\upsilon)/E$ is ascribed to different metallurgical conditions (i.e., texture) in these test strip locations.

Due to crystallographic anisotropy, different elastic constants are to be expected for different crystal orientations. The bulk elastic constants commonly used in engineering analyses are the average elastic response of many grains with different orientations, and may differ appreciably from the constants for a particular orientation sampled by the x-ray diffraction measurement. For example, the plate material strain gage tests gave an E of $207.*10^3$ MPa, and a Poisson's ratio of 0.28. These bulk properties would give a $(1+\upsilon)/E$ factor of $6.19*10^{-6}$, which is significantly different from the data given above.

X-Ray Residual Stress Results

The Y direction residual stresses in the longitudinal L1 specimen were measured at two thicknesses, while stresses in the transverse T1 specimen were measured at one thickness as shown in Table 3. Due to unbalanced residual stresses, the L1 specimen did not remain flat when machined to the thickness used for the second set of x-ray measurements. Since the x-ray equipment needed a flat surface, a stiffener was clamped to the specimen which held the specimen flat to within about ±2 mm. This amount of curvature could result in surface stress errors of about ±28 MPa.

The factors from the x-ray calibration beam "1" plate and weld regions were applied to the respective experimental residual stress data from specimens L1 and T1 to produce the data shown in Figs. 3 and 4. The x-ray equipment software reported errors of about ± 5 ksi for the L1 data, and ± 8 ksi for the T1 data. Based on the few instances where duplicate data were taken, the results shown in Fig. 2, and the results described by James (1987), the actual error bands are estimated to be less than one-half of the software reported error bands.

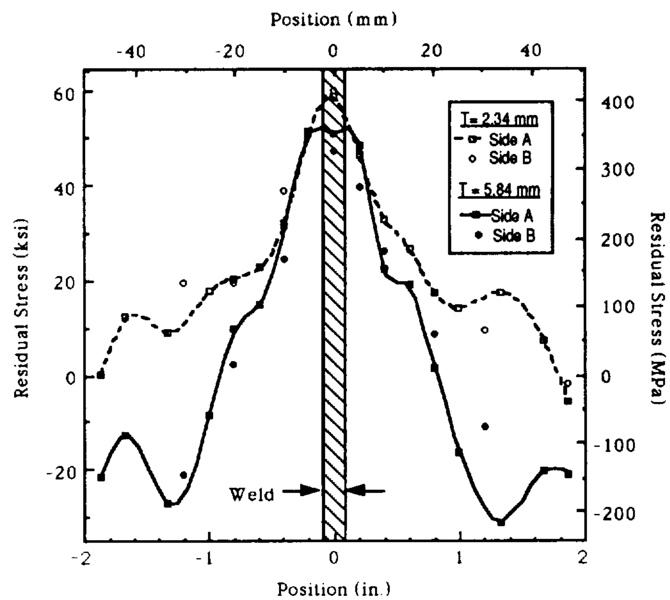

Fig. 3 X-ray residual stress data for specimen L1 measured at T=5.84 mm and T=2.34 mm.

The T1 specimen data show a large amount of scatter in Fig. 4. It is unknown whether the scatter is associated with the difficulty in measuring stresses in the weld heat-affected-zone texture (as suggested by the larger error estimates), or whether it is actual variation in the residual stresses due to the short weld distance used with this specimen.

STRAIN GAGE HOLE DRILLING MEASUREMENTS

The experimental results described here were obtained using CEA-06-062UM-120 gages made by Measurements Group, Inc. The gages were applied using the manufacturer's recommended procedures, except that no sanding was done on the chemically milled surface in order to prevent the introduction of surface residual stresses as discussed previously.

Strain gages were applied to both sides of specimens L1 and T1 at the nominal 5.8 mm thickness condition. Gages were spaced at 10.2 mm intervals, which produced hole interaction stress effects of less than 1%. Data were taken while drilling the holes in 0.13 mm increments to a depth of 1.40 mm with a milling guide and high speed air turbine assembly using carbide-tipped cutters. The gages were

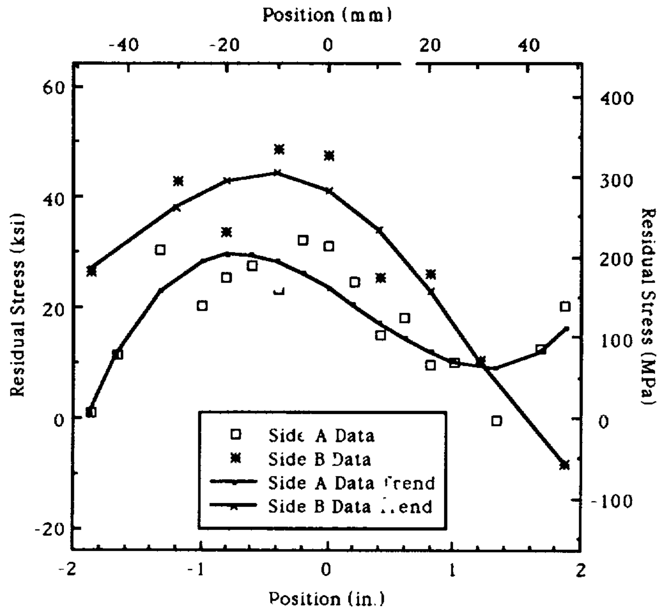

Fig. 4 X-ray residual stress data for specimen T1 measured at T=2.57 mm.

calibrated by an applied load before and after hole drilling. This procedure permitted the calculation of the strain response coefficients given in the companion paper (Hampton and Nelson, 1989) which were used to calibrate the hole drilling method for thin plates. To minimize induced strain errors from the specimen weight while in the horizontal drilling position, specimen horizontal supports were adjusted so that the strain gages indicated nearly the same strains as recorded when the specimen was aligned vertically in the testing machine.

The incremental hole drilling strain data were analyzed with the linear least squares fit method given by Schajer (1988), and described in the companion paper, to compute stresses at the surface and interior of the specimens.

As discussed in the companion paper, it was determined that the holes had an eccentricity to the gage pattern of up to 0.02 mm, which implies possible errors in the computed stresses of about 6% based on equations given by Ajovalasit (1979).

Interior Stresses from Strain Gage Data

The interior welding residual stresses (at the subsequent thickness used for the x-ray measurements) can be estimated by using the best-fit linear equations of stress from the strain gage near-surface data. However, a correction is needed to compare the predicted stresses with the x-ray stress measurements after the specimen have been machined to a thinner section, because the residual stresses in the material which was removed produced reaction stresses in the interior of the plate which are no longer reacted in the thin condition. The correction needed is computed in a similar manner to that described by Moore and Evans (1958). The forces and moments acting on the reduced section are computed by:

$$\text{Force} = \int_{\zeta_1}^{\zeta_2} \sigma(\zeta)\, d\zeta \,; \qquad \text{Moment} = \int_{\zeta_1}^{\zeta_2} \sigma(\zeta)\, \zeta\, d\zeta \qquad (1)$$

where $\sigma(\zeta)$ is the linear stress equation obtained from the strain gage analysis, ζ is measured from the neutral axis of the reduced section (always in the same direction), and the removed layers are of thickness $(\zeta_2 - \zeta_1)$. For a nonuniform stress distribution across the width, the net forces and moments are obtained by a summation which assumes the force and moment obtained from each strain gage pattern are uniform over the width interval, ΔW, midway between gage pattern centerlines. Then, the stresses at the thinner section are computed by

$$\sigma = \sigma_0 + \frac{1}{W*T}\sum(\text{Force}*\Delta W) \pm \frac{6}{W*T^2}\sum(\text{Moment}*\Delta W) \qquad (2)$$

where the + moment sign is used for the stress in the positive ζ surface, and the − sign is used for the stress in the negative ζ surface, σ_0 is the projected stress from the strain gage linear equation, $\sigma(\zeta)$, at the thinner plate surface, and T is the reduced section thickness.

The contribution from the moment term should not be included if the plate is constrained to be in the same shape (flatness) as it was when the strain gage data were obtained at the thicker condition, since then the external constrains provide the same moment effect as the removed material, and no moment correction is required. The specimen L1 and T1 x-ray data were obtained with the specimens constrained nearly flat (which matched the initial thickness condition), and therefore the moment term was not used in computing the strain gage data projected stresses at the thinner condition.

Strain Gage Residual Stress Results

The residual surface stresses obtained from the hole drilling method for specimen L1 at the 5.84 mm thickness are shown in Fig. 5. Very little difference is shown in the results for sides "A" and "B."

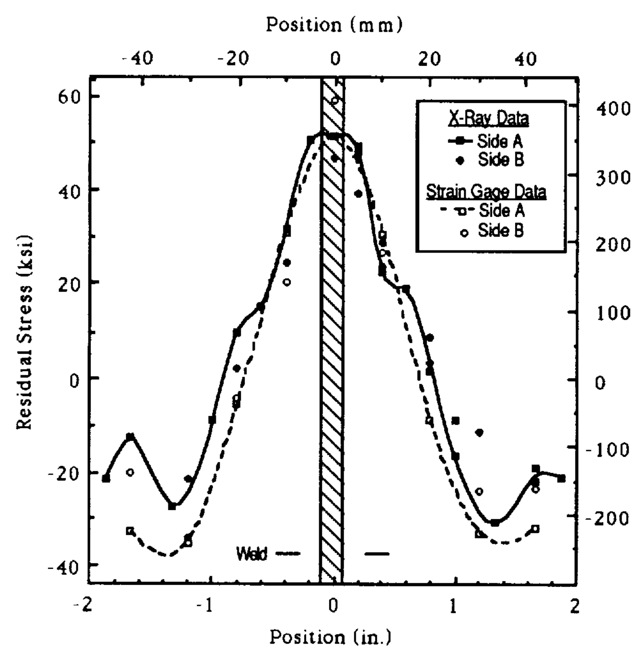

Fig. 5 Comparison of x-ray and strain gage residual stresses measured at the surface of specimen L1 (at T=5.84 mm).

The linear stress equations from the incremental hole drilling data at the 5.84 mm thickness were also used to compute residual stresses in the interior of specimen L1 (1.75 mm below each surface), where the x-ray data were subsequently obtained. Note that this is a much greater depth than is really justified, since the strain gage hole drilling data are most accurate to a Z/rm depth of about 0.4 (Hampton and Nelson, 1989), or about 0.36 mm in this case. However, if the interior stress distribution is nearly linear near the surface, this procedure may estimate the level of the interior stresses. A correction due to the net forces in the removed material of 49 MPa was computed and added to the projected stresses to obtain the results shown in Fig. 6.

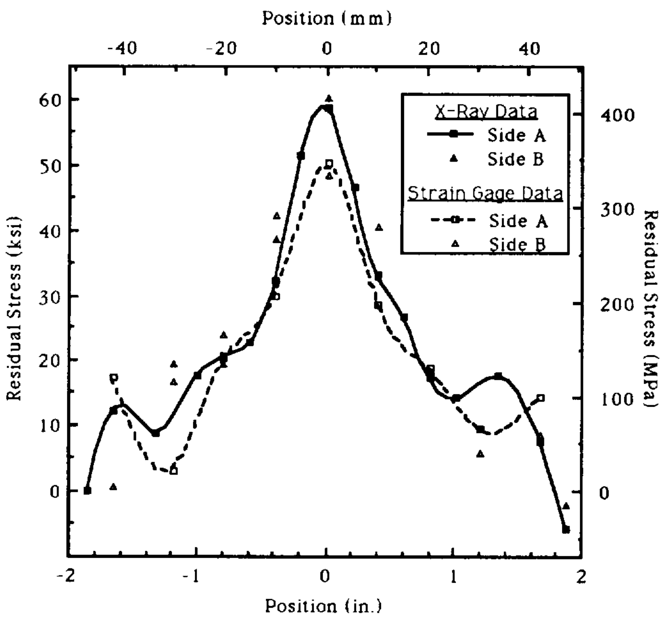

Fig. 6 Comparison of measured x-ray and projected strain gage residual stresses for specimen L1 at T=2.34 mm.

The residual stresses obtained from the hole drilling method for specimen T1 at the 5.87 mm thickness are shown in Figs. 7 and 8 for sides "A" and "B," respectively. The T1 specimen data for each side did not match, and probably reflects a very complex residual stress distribution for the short transverse welds in this specimen.

The linear stress equations from the incremental hole drilling data for specimen T1 at the 5.87 mm thickness were also used to compute residual stresses in the interior of specimen T1 (1.65 mm below each surface), where the x-ray data were subsequently obtained. This was a large extrapolation for this specimen also, and (as noted above) is susceptible to errors due to the complex stress distribution. A correction due to the net forces in the removed material of 102 MPa was computed and added to the projected stresses to obtain the results shown in Figs. 7 and 8. This projected interior stress distribution is complex, and probably not reliable at this depth below the surface of this specimen.

COMPARISON OF X-RAY AND HOLE DRILLING RESULTS

Since x-ray measurements were made at both the thick and thin thicknesses of specimen L1, comparisons can be made wit: the incremental hole drilling results at the surface and at the interior. The hole drilling surface data at the 5.84 mm thickness given in Fig. 5 shows excellent agreement with the x-ray data for both sides of the specimen. This agreement gives confidence in both the accuracy of the stress distribution, and the two independer measurement techniques. Also, the agreement of the data or sides "A" and "B" suggest that a very symmetrical residual stress distribution exists through-the-thickness of the specimen.

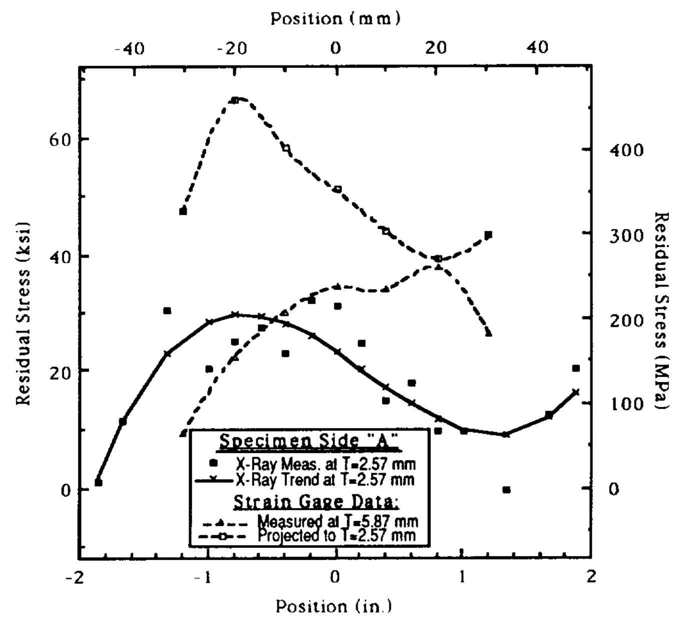

Fig. 7 Comparison of x-ray and strain gage residual stress for specimen T1, on side "A."

A comparison of the measured x-ray data and the strain gage stress data for specimen L1 which were projected 1.75 mm below the surface by the linear equation is shown in Fig. 6. The agreement of these data is also excellent considering that it is projected to a depth beyond the measured strain gage data, and that there is a significant variation in stresses with depth. Again, there is uniformity between data for sides "A" and "B," suggesting a symmetric stress distribution through-the-thickness of this specimen. Also, note that the stress distribution has a net tensile resultant, from which it is concluded that the interior of the 2.34 mm thick L1 specimen must have a net compressive resultant.

A comparison of the strain gage and x-ray measured residual stresses for specimen T1 on side "A" is shown in Fig. 7. X-ray data were only available at the thinner thickness for comparison to the hole drilling results for projected stresses at the thinner condition. The projected stresses are not in good agreement with the x-ray data. Similar results are shown in Fig. 8 for side "B."

The reason for the relatively poor results obtained for the T1 specimen is believed to be related to the existence of yield level residual stresses (as measured by the hole drilling method) in the weld

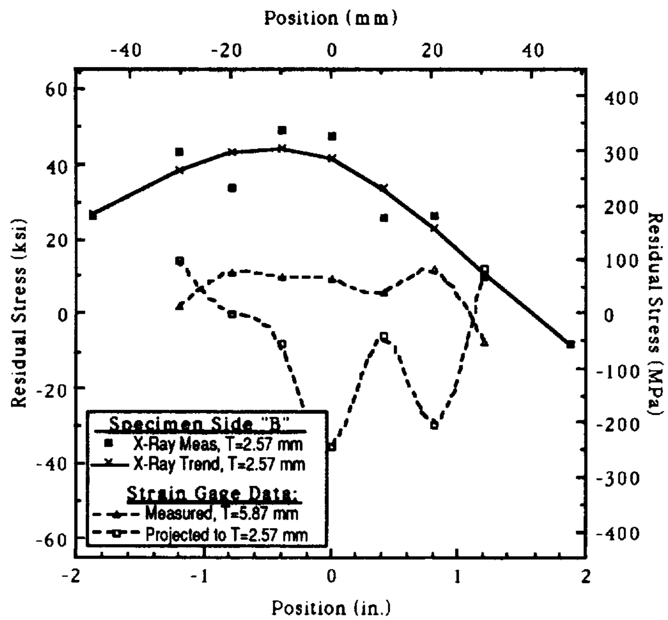

Fig. 8 Comparison of x-ray and strain gage residual stress for specimen T1, on side "B."

direction (i.e., the X direction), especially at the thinner condition. In the companion paper, experimental data are given which show that significant errors occur in hole drilling measurements of stresses in the minor stress direction (the Y stresses given in Figs. 7 and 8.) Also, errors may occur in x-ray measurements when the material is near yield levels, as shown by the calibration data in Fig. 2. By contrast, the stresses in the major principal stress direction may be in much closer agreement, as shown by the comparison between the x-ray and strain gage projections for specimen L1 in the highly stressed weld region in Figs. 5 and 6.

CONCLUSIONS

Data have been presented on the residual stresses in longitudinally and transversely welded steel plate specimens. While the longitudinal weld data have symmetry about the weld, with similar magnitudes on opposite sides, the data also show that there may be significant variations in through-the-thickness stress distributions of thin plate welds, including a probable compressive stress region in the midplane of the plate. The data on stresses in the transversely welded specimens show a great deal of nonuniformity which may be due to difficulties in obtaining uniform welds in a relatively short specimen width, as well as possible problems involving the stress measurement techniques.

The x-ray diffraction technique has been used to provide accurate residual stress data of large welded specimens made from a commonly used material. Best accuracy is obtained when the elastic constant for the metallurgical condition of interest is established by a calibration.

The incremental strain gage hole drilling method for residual stress measurement has been shown to be a useful and accurate technique for measuring surface stresses as well as stresses which vary in a linear manner in the depth direction.

When material stresses are not near the yield level, comparisons between the x-ray and strain gage hole drilling residual stress measurement methods are good. At the yield level, both the x-ray methods and the strain gage methods lose accuracy in the measurement of stresses, particularly in the minor stress direction.

ACKNOWLEDGEMENTS

The authors wish to express our appreciation for the efforts of Jeff Sakai and Jerry Yakel at the Material Engineering Labs., Naval Aviation Depot, North Island, San Diego, for their work in providing the x-ray measurements. Also, consultations with Chris Barns at NASA Ames Research Center regarding the experimental strain gage data were invaluable.

REFERENCES

Ajovalasit, A., "Measurement of Residual Stresses by the Hole-Drilling Method: Influence of Hole Eccentricity," *Journal of Strain Analysis*, Vol. 14, No. 4, 1979, pp. 171-178.

ANSI/AWS D1.1-87, *Structural Welding Code - Steel*, American Welding Society, Inc.

ASTM E 837,"Determining Residual Stresses by the Hole-Drilling Strain-Gage Method," 1985, American Society for Testing and Materials, Philadelphia, PA.

ASTM STP 776, *Residual Stress Effects in Fatigue*, American Society for Testing and Materials, 1982.

Dittman, D. L., R. W. Hampton, and H. G. Nelson, "Accelerated Crack Growth, Residual Stress, and a Cracked Zinc Coated Pressure Shell," *Int. Symposium for Testing and Failure Analysis*, ASM Int., Nov. 9-13, 1987

Hampton, R. W., and D. V. Nelson, "On the Use of the Hole Drilling Technique for Residual Stress Measurements in Thin Welded Plate," *Symposium on Nondestructive Evaluation: NDE Planning and Application*, ASME, July, 1989.

Hilley, M. E., "Principles of X-Ray Stress Measurements," Society of Automotove Engineers, Inc., Paper no. 720241, Jan. 10-14, 1972.

James. M. R., "The Use of Oscillation on PSD-Based Instruments for X-Ray Measurement of Residual Stress," *Experimental Mechanics*, June, 1987, pp. 164-167.

Kobayashi, A. S., ed., *Handbook on Experimental Mechanics*, Society for Experimental Mechanics, Inc., Prentice-Hall, 1987.

Kula, E., and V. Weiss, ed.,*Residual Stress and Stress Relaxation*, Sagamore Army Materials Research Conference Proceedings, Plenum Press, 1982.

Moore, M. G., and W. P. Evans, "Mathematical Correction for Stress in Removed Layers in X-Ray Diffraction Residual Stress Analysis," *SAE Transactions*, Vol. 66, 1958.

Nickola, W. E., "Weld Induced Residual STress Measurements Via the Hole-Drilling Strain Gage Method," ASME, (84-WA DE-25), 1984.

Nickola, W. E., "Practical Subsurface Residual Stress Evaluation by the Hole-Drilling Method," *Proc. 1986 SEM Spring Conference on Experimental Mechanics*, Brookfield Center, CT, Society for Experimental Mechanics, 1986.

Prevey, P. S., "A Method of Determining the Elastic Properties of Alloys in Selected Crystallographic Directions for X-Ray Diffraction Residual Stress Measurement," *Advances in X-Ray Analysis*, Vol 20, 1977, pp. 345-354.

Prevey, P. S., "Residual Stress Distributions Produced by Strain Gage Surface Preparation," *Experimental Mechanics*, Vol 28, No. 1, March, 1988, pp. 92-97.

Rudd, C. O., et al., "X-Ray Diffraction Measurement of Residual Stresses in Thick, Multi-Pass Steel Weldments," *J. Pressure Vessel Technology*, Vol 107, May, 1985, pp. 185-191.

Schajer, G. S., "Measurement of Non-Uniform Residual Stresses Using the Hole-Drilling Method: Part I. Stress Calculation Procedures," *Journal of Engineering Materials and Technology*, Vol 110, No. 4, October, 1988a, pp. 338-343.